Iorio, M., Marra, F., Santarelli, M., & González-Benito, J. (2021). Reinforcement-matrix interactions and their consequences on the mechanical behavior of basalt fibers-cement composites. Construction and Building Materials, 309, 125103.

DOI: https://doi.org/10.1016/j.conbuildmat.2021.125103

REINFORCEMENT-MATRIX INTERACTIONS AND THEIR CONSEQUENCES ON THE MECHANICAL BEHAVIOR OF BASALT FIBERS-CEMENT COMPOSITES

M. Iorio[a], F.Marra[b], M.L. Santarelli[b*] and J. González-Benito[c*]

[a]Laboratorio Analisi Superfici, INFN Roma Tre, Via della Vasca Navale 84, 00146 Rome, Italy.

[b]Sapienza-Università di Roma, Dipartimento di Ingegneria Chimica Materiali Ambiente. Via Eudossiana 18, 00184 Rome, Italy.

[c]Universidad Carlos III de Madrid, Departamento de Ciencia e Ingeniería de Materiales e Ingeniería Química, IQMAAB, Avda. de la Universidad 30, 28911 Leganés, Spain.

[*] Corresponding author at: Sapienza-Università di Roma, Dipartimento di Ingegneria Chimica Materiali Ambiente. Via Eudossiana 18, 00184 Rome, Italy and at Universidad Carlos III de Madrid, Departamento de Ciencia e Ingeniería de Materiales e Ingeniería Química, IQMAAB, Escuela Politécnica Superior, Avda. de la Universidad nº 30, 28911 Leganés (Madrid), Spain

E-mail address: marialaura.santarelli@uniroma1.it
javid@ing.uc3m.es
Telephone number: +39 06 4458 5561 +34 91 624 88 70

Abstract

In order to prepare basalt fibers-reinforced cement-based mortars with higher compatibility between reinforcement and matrix, basalt fibers with new surface treatments (sizing) were studied looking for enhanced interaction at the interphase between basalt fibers and cement matrix. As-received, calcinated, activated and silanized (by three silane aqueous solutions: i) γ-aminopropyltriethoxysilane, APTES; ii) γ-aminopropylmethyldiethoxysilane, APDES and iii) a mixture APTES+APDES 50% by weight) basalt fibers were dispersed in Portland cement matrix. Performances of the composites were evaluated by mechanical tests. Final correlation between the fibers surface characteristics and mechanical performance was carried out considering the induced microstructural changes and adhesion at the interface. Fractographic analysis by SEM and laser and

optical profilometry were performed. A clear improvement in mechanical properties was obtained when basalt fibers were dispersed in cement matrix. Results suggest that better behavior is achieved when basalt fibers modified with a complex mixture of silanes are dispersed in cement matrix.

Keywords: basalt fibers, surface treatments, cement matrix, interphases.

1. INTRODUCTION

Portland cement, developed in the mid nineteenth century, became the preferred material in architecture. Portland cement-based materials have the advantages of being widely available, relatively inexpensive compared to many other materials and usually have stiffness and thermal expansion compatible with the material to be repaired, being relatively easy to apply and cure.

However, its relatively high modulus and low tensile strength can create sometimes structural problems in its application. Furthermore, other disadvantages are related to the interaction with some aggregates, the weathering and to the shrinkage cracking phenomena [1,2].

A possible approach to reduce these defects may be the use of short and randomly dispersed fibers because it is expected from them to transmit properly stresses to the matrix and reduce crack openings. In addition, fibers may act like attachment points on cracks, making difficult their propagation [3]. Therefore, fiber reinforcement limits the diffusion of shrinkage cracking by decreasing the width of the cracks. Indeed, the presence of the fibers can improve properties such as tensile, flexural, impact, fatigue and abrasion strength, elongation at break and toughness in composite materials. Especially, one of the major roles of the fibers in concretes and mortars is to increase the fracture energy, which is directly related to cracks formation and propagation [4].

The effectiveness of fibers to improve the fracture energy depends on the composition of the composite, aspect ratio and nature of the fibers, the nature of the matrix and the physico-chemical interactions between fibers and the matrix among other factors [3,4]. Generally, the relative amount of fibers used in these materials is limited to 1–3% by volume but using this low amount of fibers

only an improvement in terms of fracture toughness of concretes and mortars is expected in most of the practical cases. Mechanical strength of the whole material can be increased when higher mass of fibers is used [3,5–7]. Furthermore, since the size and aspect ratio of fibers influences the crack formation and propagation, some important issues should be considered in this sense. Indeed, in a cementitious material, the matrix cracking occurs first at the micro level, consequently the presence of short and relatively closer fibers acts on the microcracks avoiding the coalescence in macrocracks. Although large fibers (up to 50 or 80 mm) may stop macrocracks propagation, they only contribute to increase toughness with a relatively small improvement of the composite strength. Furthermore, short fibers can enhance the strength of the resulting material providing a little improvement in post-peak toughness because they have to be pulled out after that macrocracks are being propagated [2,8]. The fiber-matrix interactions directly influence the mechanical properties of the cementitious composite since the fiber-matrix interphase is the region of the material which conditions the ability of fibers to transfer loads to the matrix and stabilizes cracks propagation. Indeed, if fiber-matrix interactions are too low, no continuity along the composite material is present, being responsible for its weakness [9].

Consequently, a good adhesion or adequate physico-chemical interactions between fiber and matrix should be achieved in order to avoid failure mechanisms that could occur at the interface such as debonding, pull-out, fiber sliding and crack bridging phenomena. These phenomena have a significant influence on the total energy consummation during crack propagation and they can be controlled by fiber reinforcements [5,10,11].

In order to enhance fiber-matrix interfacial adhesion, several methods have been proposed. Among them, modification of fiber surfaces through chemical treatments is one of the most used [11,12].

Various types of fibers have been used to reinforce mortars and concretes. A well-known example is the addition of asbestos fibers for reinforcing building material. However, since 1970 its use decreased due to the risk to human health associated to fiber breathing [6]. Other types of fibers used as reinforcement are [2]: steel, glass and carbon fibers, synthetic polymeric fibers (such as

polypropylene, polyethylene and polyolefin, polyvinyl alcohol (PVA) etc.) and natural vegetable fibers (applied only in ordinary concretes and not in high performance structural concrete). Vegetable fibers show disadvantages under humid and alkaline environments leading to reduction in strength and toughness of the cement matrix [13].

Currently, a great interest is rising in the use of basalt fibers for their good compatibility with cement materials. Basalt fiber represent an economic and sustainable alternative to the other type of fibers [7,12,14].

It is referred that when adding fibers in concrete and mortars an increase in the mechanical properties and a reduction of the shrinkage phenomenon could be achieved [7,14]. Branston et al. [15] have found that the presence of basalt fibers clearly increases pre-cracking strength. Jiang et al. [16] showed that adding chopped basalt fibers to a cement matrix, tensile strength, flexural strength and toughness index were improved, while compressive strength did not increase significantly. High et al. [17], studying the use of chopped basalt fibers for concrete structures, have found that the fibers enhanced the flexural modulus but they had only a little effect on the compressive strength. However, several studies stated that better performance of basalt fiber-reinforced cement composites can be achieved by improving the fiber-matrix interphase through surface treatments (referred as sizing treatments) of the fibers [18,19].

A reduced number of case studies about new surface treatments of basalt fibers for improving matrix-reinforcement adhesion in cement-based materials is available. In this regard, the aim of the present work is to improve the performance of cement-based materials by optimization of fiber-matrix interphase through new fibers surface treatments.

2. EXPERIMENTAL

2.1 Materials

In this study, the binder used to prepare mortar samples was a Portland cement PII/A-L 42.5 R according to European Standard EN-197 [20]. It was provided by Cementos Portland Valderrivas

(Madrid, Spain). As aggregate, a siliceous sand, with a grain size between 0.2-0.5 mm, supplied by Arenas Silíceas Gómez Vallejo (Segovia, Spain) was used. Basalt continuous filament (mean diameter 17 μm) chopped to a length of about 6.4 mm with a sizing compatible with cement matrix was supplied by Incothelogy GmbH. A chlorhydric acid aqueous solution (37% wt), Sharlab, and two silanes, γ-aminopropiltriethoxysilane (APTES) and γ-aminopropilmethyldiethoxysilane (APDES), supplied by ABCR GmbH & Co.KG, were used to prepare pre-treated and silane coated basalt fibers.

2.2 Sample Preparation

Mortar samples were prepared with a binder/aggregate ratio of 1:2. Distilled and deionized water was used in a water/binder ratio of 0.45. In order to obtain the composites, as-received or modified basalt fibers were added to the reactive mixture at 1% by weight. As-received or commercial fibers were subjected to surface pretreatment processes: i) calcination (elimination of the original silane sizing with heating treatment) and ii) activation (calcinated fibers were immersed in hydrochloric acid solution to regenerate silanol groups, Si-OH, on the fiber surface to allow the grafting of the new sizings). After the activation pretreatment, the fibers were washed with deionized and distilled water to eliminate acid residues and finally dried. Subsequently, the activated fibers were subjected to a silanization process. In particular, the fibers were chemically treated with three different aminosilane aqueous solutions: i) γ-aminopropyltriethoxysilane, APTES; ii) γ- aminopropylmethyldiethoxysilane, APDES and iii) mixture 50% by weight of both silanes, APTES + APDES.

The methods used to modify basalt fibers are described more in detail in reference [12]..

In order to ensure the effectiveness of the surface treatments, changes in the structure of the surface were studied by Fourier transformed infrared spectroscopy, FT-IR, reported in the same reference [12].

Furthermore, the standard UNI EN 196-1:2005 [21] was used as a guide for the preparation of mortar samples. Mixing was done in a standard mixer (IIC S.A., *Amasadora Automàtica Multinorma*). The

process started mixing the cement and water for 30 s at low agitation speed. After that, the aggregate was added, blending for 90 s at high speed. Finally, fresh mixtures were cast in 20 × 20 × 80 mm silicon molds (Figure 1). Molds were half filled and compacted to avoid voids formation. Afterward, a second layer of mixture was poured, and the sample was compacted again.

Samples were cured and tested according to the standard UNI EN 1015-11:2007 [22]. Specimens were prepared by subjecting the mixture at 25 ºC and 95±5% of relative humidity, RH, for 7 days in the polyethylene bags (Figure 2b). Finally, the specimens were stored in a climatic chamber for 21 days at 25 °C and RH 65±5% (Figure 2c) before performing the mechanical tests. Therefore, the specimens were tested 28 days after their preparation and immediately after they have been removed from the curing conditions as the UNI EN 1015-11:2007 states.

In the Table 1 are gathered the samples codes and the components of the corresponding mixtures (six specimens were prepared for each mixture).

Table 1. Sample codes of the cement-based mortars prepared and components of the mixtures

Code	*Binder/Aggregate (Cement/Sand)*	*Water/ Binder*	*Fibers % by weight*	*Basalt Fibers Surface Treatment*
REF CEM	1:2	0.45	--	--
ASR + CEM	1:2	0.45	1%	*AS-RECEIVED* (commercial silane sizing)
CAL + CEM	1.2	0.45	1%	*CALCINATION* (heating process)
ACT + CEM	1:2	0.45	1%	*ACTIVATION* (hydrochloric acid solution)
APT + CEM	1.2	0.45	1%	*SILANIZATION* (γ-aminopropiltriethoxysilane, APTES aqueous solution)
APD + CEM	1:2	0.45	1%	*SILANIZATION* (γ-aminopropilmethyldiethoxysilane, APDES aqueous solution)
APTAPD + CEM	1:2	0.45	1%	*SILANIZATION* (mixture 50% by weight APTES+APDES)

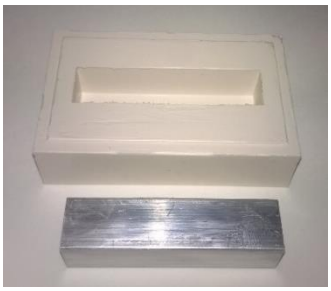

Figure 1. 20×20×80 mm silicon molds.

Figure 2. Mixing (a) and curing (b-c) of cement-based mortar samples.

2.3 Instrumental techniques

2.3.1 Scanning Electron Microscopy (SEM)

In order to investigate the interaction between as-received and modified fibers with cement matrix, the fracture surfaces of specimens obtained after performing the three point flexural tests were inspected by scanning electron microscopy using a TENEO field emission scanning electron microscope, FESEM (FEI). The acceleration voltage was 4.0 kV and 5.0 kV and the T1 detector was used taking the signal coming from backscattered electrons. Considering that the samples are not conductive, they were sputter coated with gold using a low vacuum coater Leica EM ACE200. SEM images were collected at different magnifications to obtain information about the dispersion of the fibers in the matrix (120×), the adhesion of the matrix to the fiber surface and to study the fiber-matrix interphase (2000× and 3500×). SEM observations were carried out on small regions of only one of

the facture surfaces of the specimens. A representative specimen for each mixture showing similar flexural and compressive strength values compared to the other ones, was selected for the investigation.

2.3.2 Surface Profilometry Measurements

In addition to the SEM observations, another fractographic analysis of the composite materials was carried out by laser and optical profilometry considering their information at different scale.

- Laser Profilometry

  Laser profilometry was carried out using a Talyscan 150 (Taylor-Hobson) instrument. The 3D topographic images of the composite materials were evaluated for studying the whole heterogeneity and irregularities of the fractured surfaces (e.g voids due to the pull-out of the fibers, cracks, height differences on fracture profile).

  Three surfaces for each sample were analyzed in order to obtain averaged data. An area of about 20 mm × 20 mm was scanned at 2500 μm/s taking horizontal profiles with a linear resolution of 5 μm, spacing between profile was 20 μm.

- Optical Profilometry

  Optical profilometry was performed using an OLYMPUS DSX 500 instrument to evaluate heterogeneities and irregularities at higher magnification (10× magnification). Three surfaces for each sample were analyzed in order to obtain averaged data. The investigated area (1994 μm × 1994 μm) was chosen in five different regions of each fractured surface (one in the center and four near the corners).

2.3.3 Atomic Force Microscopy (AFM)

Roughness studies of as-received and modified fibers surfaces were performed by atomic force microscopy, AFM, using a microscope Multi-Mode Nanoscope IVA (Digital Instruments/Veeco Metrology Group). The measurements were conducted at ambient conditions in tapping mode with antimony doped silicon probe (force constant, k = 1-5 N/m). The frequency was set to the resonant frequency of the probe close to the surface of the sample to be analysed. The initial amplitude of the probe oscillation and set-point amplitude for AFM imaging were chosen to maximize the image contrast.

Arithmetic average of the absolute values of the roughness profile, R_a, and the root mean square average of the roughness profile, R_q, were obtained to study the topography at nanoscale. Due to the heterogeneity of the fibers surfaces, the roughness was calculated in several representative regions of the fiber surface: a) smooth areas and b) areas with a high amount of sizing (red squares in Figure 3). A 2nd order flatten was used before estimate surface roughness parameters.

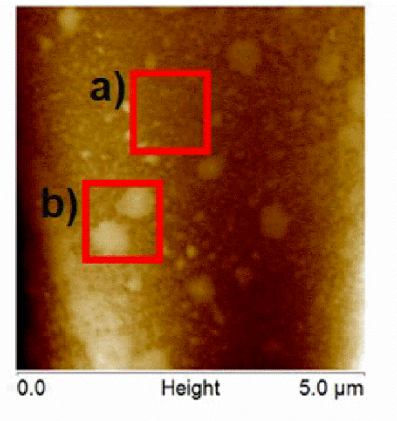

Figure 3. AFM Height Image of as-received basalt fibers: a) smooth areas; b) areas with a high amount of sizing.

3. RESULTS

3.1 Mechanical tests

3.1.1Mechanical Tests

Mechanical tests were performed according to standard UNI EN 1015-11:2007 using a MICROTEST EM2/200/FR (Madrid, Spain) universal testing machine. Three-point flexural tests and compressive tests were carried out on six specimens for each type of sample.

For three-point flexural test a 5 kN load cell was used. The support span was set at 50 mm and the load was applied with a rate of 2 mm/min. Cubic portions (20×20×20 mm) of each specimen resulting from the fractured specimens after the three point flexural tests, were mechanical tested by compression using a 20 kN load cell and applying the load at rate of 2 mm/min.

Finally, the flexural and compressive strength data were statistically treated using Weibull distribution function (see Appendix A in Supplementary Material) that is one of the most widely used to describe the fracture strength of ceramics [23,24, 27]. The results from mechanical test were obtained following the formulations in […].

- *Three-point flexural strength tests*

In Figure 4, the flexural stress-strain curves for the prepared mortars is observed. A complete description of all images of fractured specimens is shown in Figures S1-S7 in Supplementary Material.

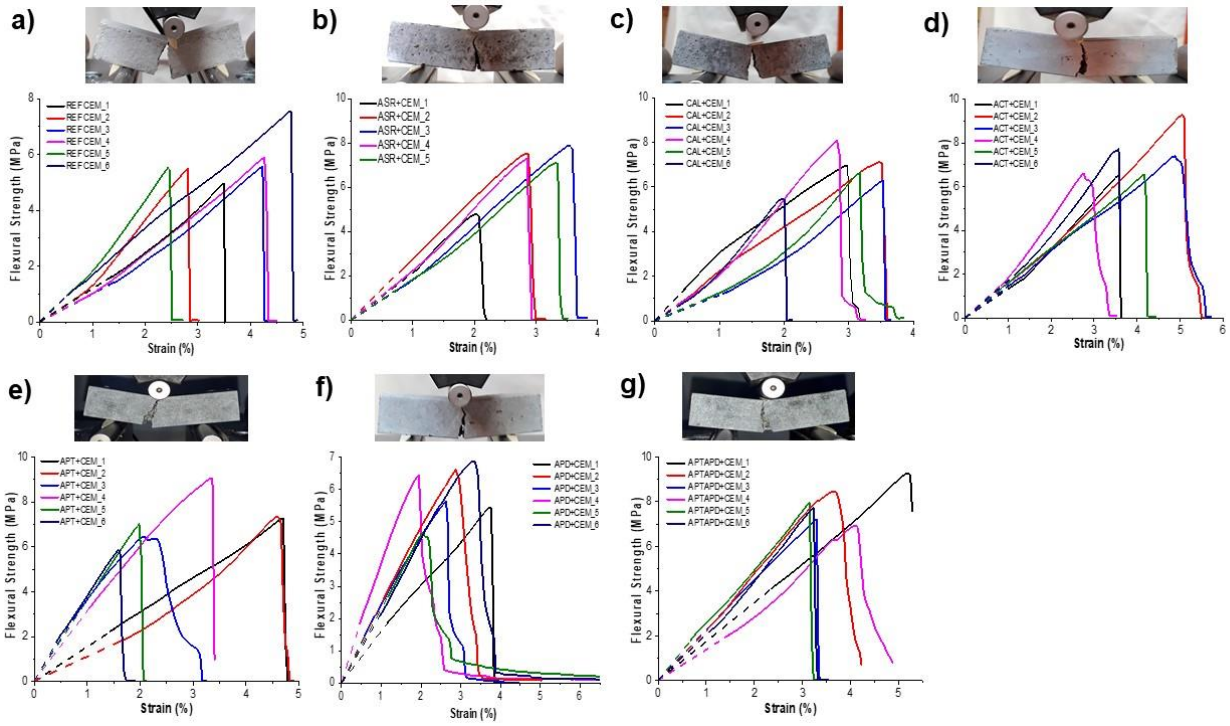

Figure 4. Images of fractured specimens of REF CEM samples and flexural *stress-strain* curves: a) REF CEM samples; b) ASR+CEM samples; c) CAL+CEM samples; d) ACT+CEM samples; e) APT+CEM samples; f) APD+CEM samples; g) APTAPD+CEM samples.

Considering the fracture behavior of the samples tested for the neat mortar, more homogeneous fracture is observed leading to complete separation between the two pieces resulting from the fracture (Figure 4a). However, the region of fracture for the samples reinforced with the fibers (Figures 4b-f) point out more tortuous crack development and the pieces resulting from the tests after the corresponding fracture have not completely separated each other.

The flexural strength plots suggest that specimens containing fibers failed in the same brittle manner as the neat mortar (REF CEM). Only slight differences are observed for samples containing modified fibers (Figure 4b-f).

In order to study possible changes between each group of samples, a deeper analysis of the three-point flexural test data was done. For instance, the flexural strength (σ_f) values obtained for each batch were discussed according Weibull distribution, using the Grubbs approach [28].

The statistical properties of the averaged flexural strength values for the different composites applying Weibull statistics are summarized in the Table 2.

Table 2. Parameters obtained after the Weibull fitting of the data obtained from the three-point flexural tests.

Samples	***Averaged Flexural Strength, σ_f (MPa)***	***Weibull Characteristic Strength, σ_0 (MPa)***	***Weibull Modulus, m***	***Correlation, (r)***
REF CEM	5.8	6.4	6.1	0.80
ASR+CEM	7.5	7.6	28.7	0.97
CAL CEM	6.8	7.1	9.0	0.97
ACT+CEM	7.3	8.0	7.5	0.76
APT+CEM	7.2	7.6	7.7	0.87
APD+CEM	6.0	6.3	8.1	0.96
APTAPD+CEM	7.9	8.3	10.8	0.91

Considering the Weibull analysis, a quite good linear relationships between ln ln [1/(1−P)] and ln σ, in the most of cases are observed. Therefore, it can be considered that the σ_f values obtained are statistically significant and the Weibull distribution fit is reliable. Poorer observed fits might be ascribed to the presence of pores and microcracks with various orientations. Besides, the Weibull moduli obtained are within the range of values found for other similar ceramic materials [26]. High Weibull moduli associated to narrow strength distributions are usually desirable, because a material with high Weibull modulus is more predictable in terms of its mechanical failure, being less likely to break at a stress much lower than a mean value.

Furthermore, the obtained Weibull characteristic strength values, σ_0, are comparable to the mean flexural strength values obtained experimentally for each sample.

Furthermore, toughness was evaluated by integrating the total area under the flexural stress-strain curve to determine a possible effect of the fibers. In this work, the post-cracking behavior was also considered for the toughness determination. Moreover, the flexural modulus, *E* and the elongation at break, ε were determined in order to define the rigidity and brittleness of the materials respectively. Averaged values of the results obtained for each sample are given in the Table 3.

Table 3. Flexural parameters of the studied cement-based mortar samples.

Samples	***Flexural Strength, σ_f (MPa)***	***Flexural Modulus, E (MPa)***	***Toughness (MPa)***	***Elongation at Break, ε (%)***
REF CEM	5.8	180	1041	3.7
ASR+CEM	7.5	257	1210	3.1
CAL CEM	6.8	252	997	3
ACT+CEM	7.3	206	1535	4
APT+CEM	7.2	263	1224	3
APD+CEM	6.0	222	1066	2.7
APTAPD+CEM	7.9	228	1592	3.8

It can be observed that there is always an increase of flexural strength (σ_f) and flexural Modulus (E) when fibers are added to the mortar.

The APD+CEM sample shows a flexural strength value similar comparing with the neat mortar datum. Instead, the samples containing as-received, activated and silanized with APTES (APT) or the mixture APTES+APDES (APTAPD) basalt fibers present the highest values of σ_f. Consequently, data suggest that a surface treatment is responsible of a better adhesion with the matrix enhancing the resistance of the whole material.

However, the use of only the difunctional silane does not seem to be enough as to alter the flexural mechanical behavior of mortar. Regarding our results only when the trifunctional silane is used the mechanical performance is enhanced, being even improved if a more opened chemical structure is generated at the interphase with the addition of the difunctional silane as described in previous papers

of the authors [12,29] and it is showed in Figure S8. In fact, the APTAPD+CEM sample showed the highest value of the flexural strength.

APTAPD+CEM and ACT+CEM samples showed the highest flexural toughness values. In these cases, higher toughness is related to higher resistance to crack propagation. Probably, in the case of ACT+CEM and APTAPD+CEM samples, the presence of high number of OH groups and/or easier accessibility to those OH on the fibers, might be responsible of better interaction with the cement matrix preventing fiber sliding respect to the matrix during mechanical test and even after material fracture had occurred. In addition, the presence of NH_2 groups in the molecular chains of the silanes can contribute to reinforce the interaction between matrix and concrete. As already confirmed by infrared spectroscopy [12], this higher number of OH groups on the modified fibers was due to: in one case, the activation treatment performed on the fibers surface to regenerate hydroxyl groups after calcination process and, in the other case, the high amount of non-condensed silanol groups when the three-functional silane (APTES) was used to coat the fibers. For the other samples, the toughness values are not significantly different than the neat mortar.

Considering the flexural modulus, E, it increases when adding fibers to the cement matrix, in accordance with the higher modulus of the basalt fibers respect to the cement matrix. Furthermore, considering the values of elongation at break, ε the samples APTAPD+CEM and ACT+CEM are less brittle than the others pointing out another possible contribution to their higher toughness.

In conclusion, a better compatibility is achieved using the APTES+APDES basalt fibers in cement matrix (APTAPD+CEM sample).

- *Compressive strength test*

About the compressive behavior, the corresponding statistical properties obtained by Weibull statistical analysis are summarized in the Table 4.

Table 4. Parameters obtained after the Weibull fitting of the compressive strength tests data.

Samples	***Averaged Compressive Strength, σ_c (MPa)***	***Weibull characteristic strength, σ_0 (MPa)***	***Weibull modulus, m***	***Correlation (r)***
REF CEM	29.1	30.6	10.2	0.80
ASR+CEM	23.4	25.2	7.3	0.94
CAL+CEM	30.6	33.4	6.0	0.94
ACT+CEM	36.6	40.4	5.2	0.99
APT+CEM	31.9	35.0	5.8	0.85
APD+CEM	26.6	29.5	4.4	0.94
APTAPD+CEM	31.9	34.7	5.2	0.91

As observed in flexural strength results, a good linear fit was also obtained for the compressive strength results. Consequently, the compressive strength experimental data can be also described with the Weibull distribution function, being the compressive strength values statistically significant.

In order to deepen the compressive behavior of the studied mixtures, other important mechanical parameters were considered as well.

Compressive strength, σ_c, Modulus, *E,* toughness (evaluated considering the area below the compressive curves until the maximum compressive strength value) and elongation at break, ε, were estimated and summarized in Table 5. The compressive strength curves for all the specimens tested are shown in Figure S9 (Supplementary Material).

Table 5. Mechanical parameters obtained from the analysis of the compressive curves of the cement-based mortar samples.

Samples	***Compressive Strength, σ_c (MPa)***	***Compressive Modulus, E (MPa)***	***Toughness (MPa)***	***Elongation at Break, ε (%)***
REF CEM	29.1	1062	5683	3.4

ASR+CEM	23.4	1091	3420	2.9
CAL CEM	30.6	1482	3885	2.6
ACT+CEM	36.6	1755	4822	2.7
APT+CEM	31.9	1308	4852	3.1
APD+CEM	26.6	1500	2985	2.2
APTAPD+CEM	31.9	1445	4407	2.8

About the compressive strength, slightly higher values were obtained for samples containing activated (ACT+CEM) and silanized APTES (APT+CEM) and APTES+APDES (APTAPD+CEM) basalt fibers, in accordance with those obtained from the flexural tests.

Respect to REF CEM the compressive modulus, *E,* increases for all samples containing fibers, except when commercial fibers are used. The elongation at break, ε, decreases. Therefore, as compression mechanical behavior, the introduction of fibers leads towards a little more rigid and brittle materials. The unexpected value of the modulus of as-received fibers (ASR+CEM sample) can be explained with a different disposition of this fibers respect to the silanized fibers Indeed, the sizing of the commercial basalt fibers makes them very flexible and can organize themselves in random coil form without conferring the opportune resistance in terms of rigidity to the whole material because of non-proper load transfer (Figure 5a). On the contrary, the proposed surface treatments make the fibers less flexible as can be clearly seen when they are handled. This suggests that when they are mixed with the components of the mortars, they remain in their more extended form, being more separated each other and consequently leading to more effective reinforcement (Figure 5b).

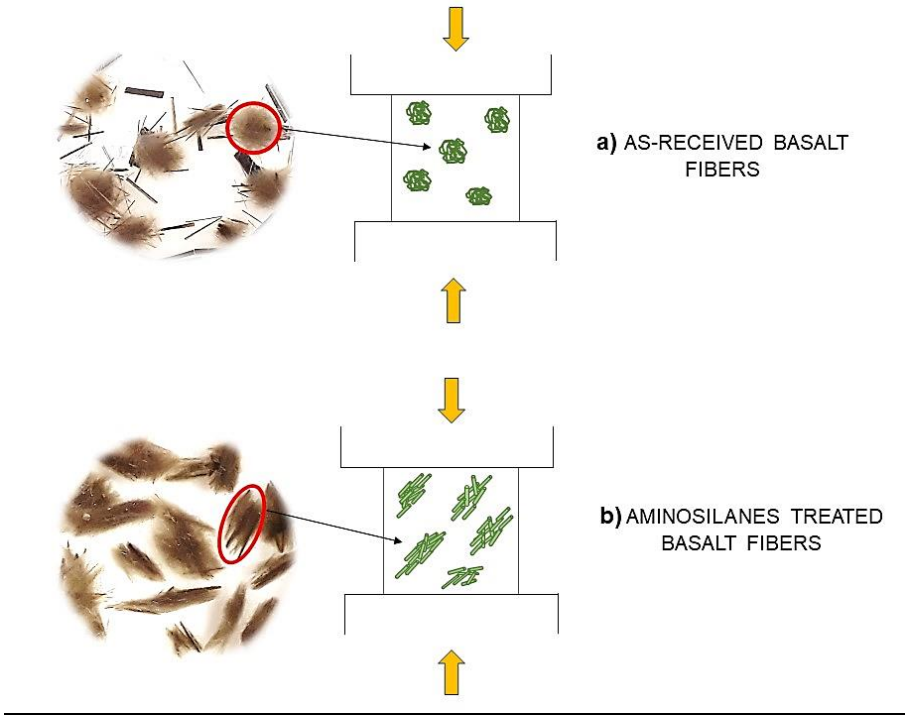

Figure 5. Photographs and schemes of a) as-received and b) aminosilanes treated basalt fibers after stirring with water, in order to help describing compressive behavior.

In addition, the sample containing as-received fibers (ASR+CEM) shows slightly lower values than the neat mortar. These results are in accordance with other studies, showing that commercial fibers do not increase significantly the compressive strength [16,17].

Toughness in terms of compression resistance decreases for all samples with fibers respect to the neat mortar (REF CEM). Therefore, there is only a small contribution due to the modulus increase correlated to the incorporation of fibers.

3.2 Fractographic analysis

3.2.1 Scanning Electron Microscopy (SEM)

Fracture surfaces were observed by scanning electron microscopy to study the failure mechanism of the composites when they are subjected to the three-point flexural strength tests.

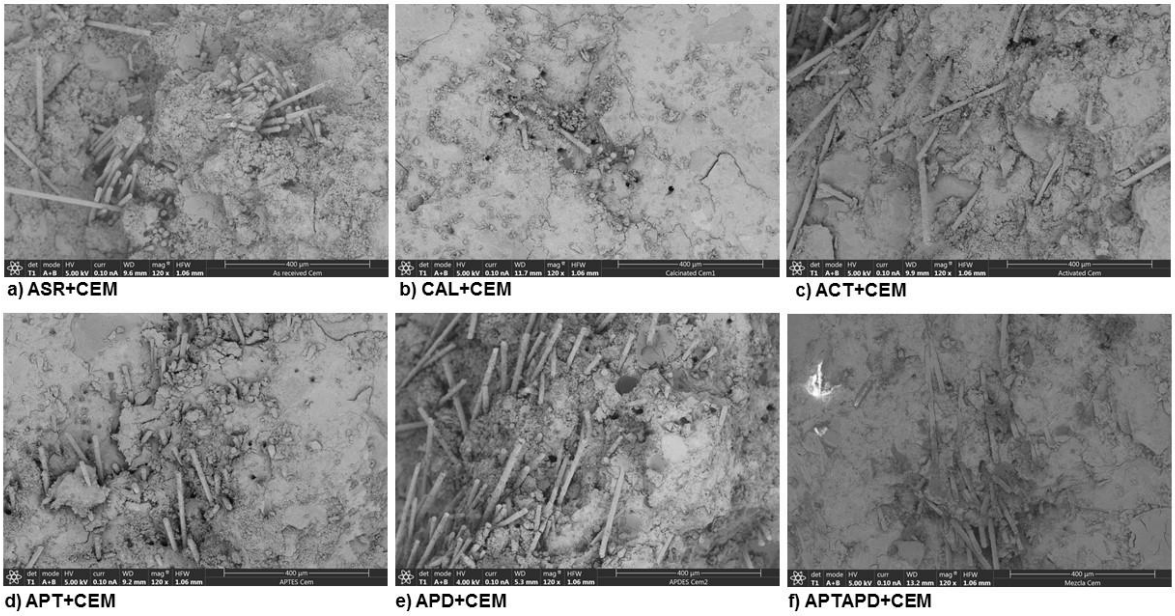

Figure 6. SEM images for all fiber reinforced mortar samples at 120× magnification.

In Figure 6 the fracture surfaces of the fiber reinforced mortar samples at 120× magnification are showed. From these SEM images, information about the dispersion of the fiber in the matrix is obtained. A heterogeneous dispersion of the fibers in the matrix and evidences of pull-out phenomena are observed for all samples. The chopped fibers appear as form of bundles in the core of the mixture. Indeed, the process of mixing did not allow separating the fibers each other in the bundle leading to the corresponding not uniform dispersion within the cement matrix.

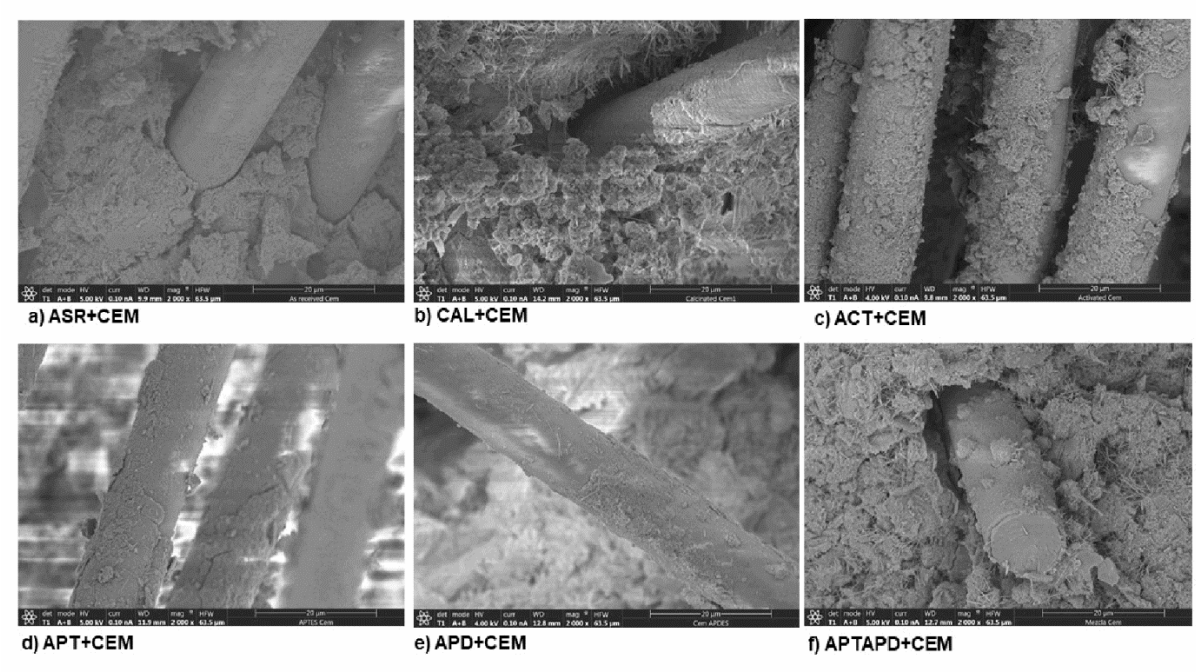

Figure 7. SEM images for all fiber reinforced mortar samples at 2000× magnification.

The SEM images at 2000× of magnification (Figure 7) provided information about the type of failure at the fiber-matrix interphase. Considering the different used fibers, the as-received fibers (ASR) and calcinated fibers (CAL) (Figures 7 a and b) showed smooth fibers surfaces, pointing an adhesive failure at the interphase. Instead, when activated (ACT) or silanized fibers (Figures 7 c, d, e and f) were used, the cement matrix adhered to the fiber surfaces, suggesting a higher contribution of cohesive matrix failure. These results underline that silanized fibers or simply activated fibers enhance adhesion between the reinforcement and the matrix as expected attending the mechanical behavior already discussed. Especially, the samples ACT+CEM and APTAPD+CEM present as more cementitious material remaining on the fibers after the failure, and the highest mechanical properties in terms of mechanical strength and toughness.

3.2.2 Surface Profilometry Measurements

- Laser Profilometry

In order to understand the failure mechanism in the neat and fiber-reinforced cement-based mortars, 3D topographic images were evaluated. Indeed, by this technique, information is obtained at a higher scale than the SEM ones. Fractographic analysis was performed on the fracture surface of the materials resulting from the three-point flexural tests. A representative 3D topographic image for each sample is shown in Figure 8.

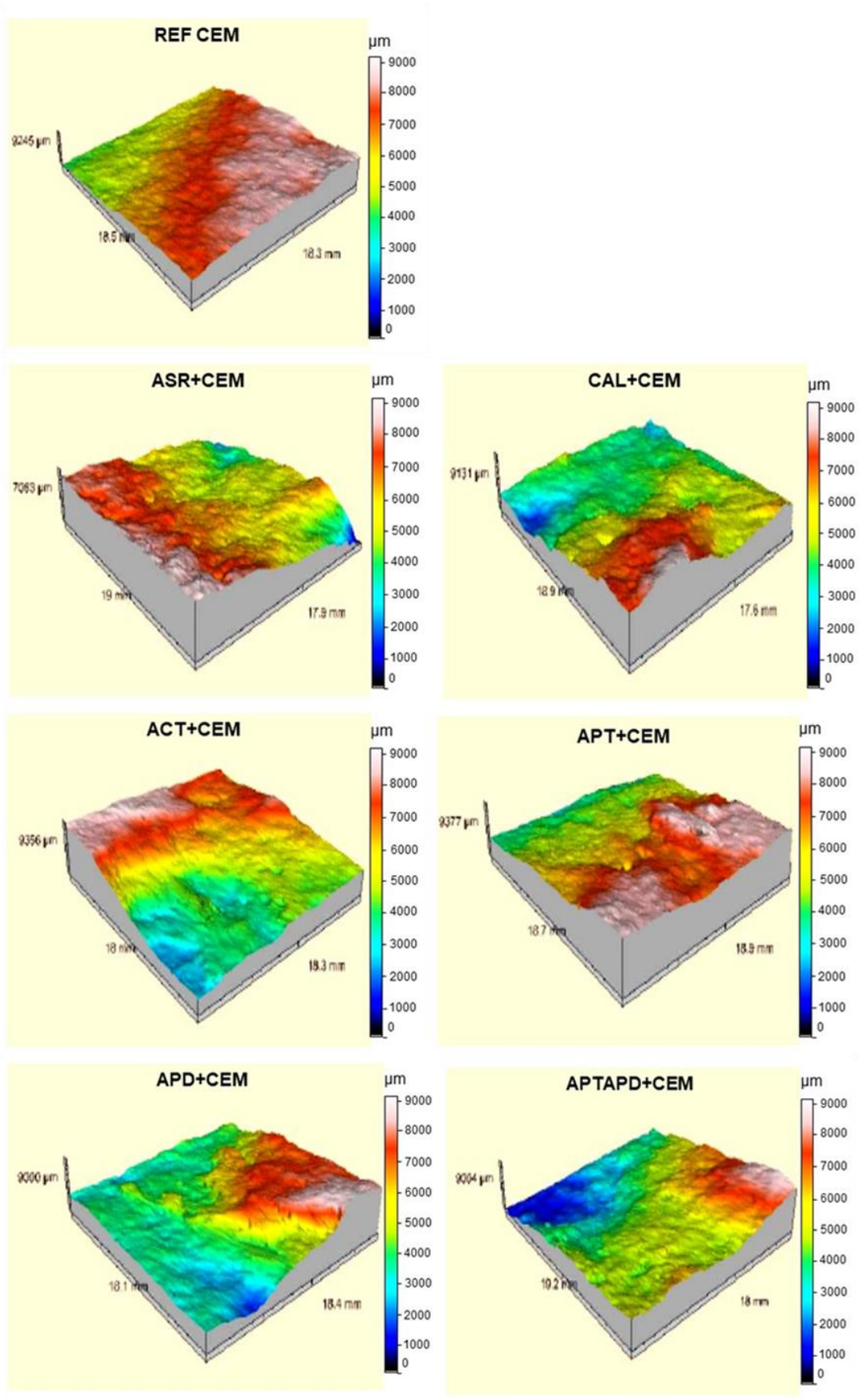

Figure 8. Representative 3D topographic images (20 mm × 20 mm) of fracture surfaces of the studied cement-based mortars.

Considering the 3D topographic images of the fracture surfaces (Figure 8), the neat sample (REF CEM) shows a smoother fracture surface than the other samples with fibers. Indeed, more tortuous fracture surfaces are evident for the mortars containing fibers. Commonly, studies about the influence of aggregate size indicate that tortuous fracture surfaces denote a less brittle behavior in concrete and mortars [30]. Consequently, in the studied samples, the presence of the fibers produces a less brittle behavior related to the topographic heterogeneity and in accordance with the mechanical results. The presence of the fibers and the nature of their surface affect the interphase adhesion with the matrix and the fracture mechanism, directly influencing the final fracture surface of the whole materials.

- Optical Profilometry

In order to evaluate in detail the failure mechanism at higher magnification, 3D profile images were collected by optical profilometry.

As an example, representative 3D images of all groups of investigated samples is shown in the Figure 9.

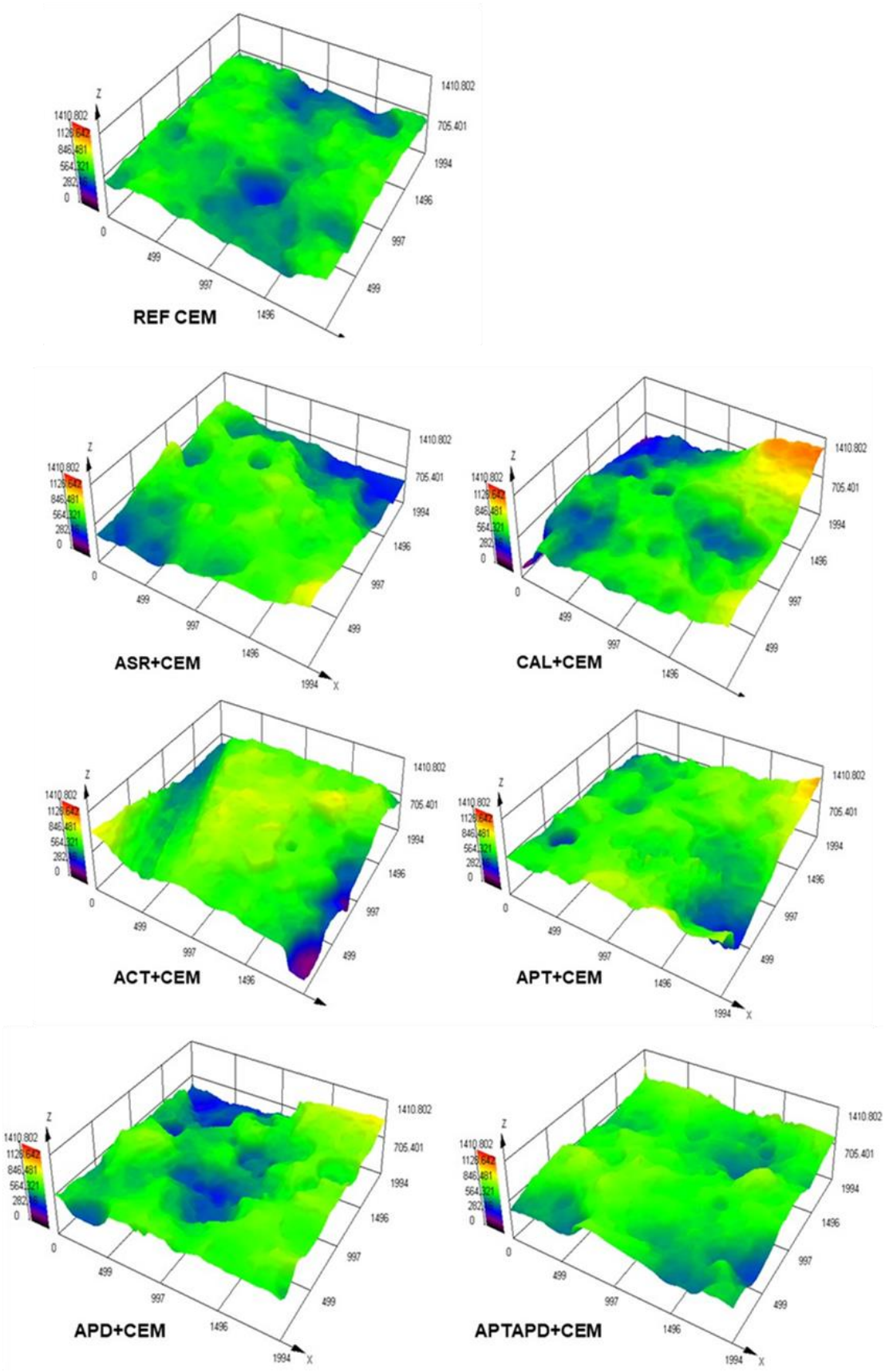

Figure 9. Representative 3D topographic images (1994 µm × 1994 µm) of fracture surfaces of the studied cement-based mortars.

In this case, the topographic characteristics (such as the presence of pores) of the fracture surfaces are more pronounced than the 3D profile images obtained by Laser Profilometry. However, the differences in surface irregularities between neat and reinforced samples are more clearly observed when a larger region corresponding to the whole fracture surface of the specimens is studied. In conclusion, optical profilometry measurements have also demonstrated that a more tortuous fracture surfaces are evident for the mortars containing fibers.

3.4 Atomic Force Microscopy (AFM)

AFM characterization of the as-received and modified fibers surfaces was done. An estimation of surface roughness at nanoscopic scale is interesting in order to evaluate possible influences on the final interactions with the matrix. From the analysis of AFM topographic images, the roughness parameters R_a and R_q of each kind of fiber were extracted (Table 6).

Table 6. Roughness parameters (R_a and R_q) obtained for as-received and modified basalt fibers.

	R_a (nm)	**R_q (nm)**
AS-RECEIVED	2.2 ± 1.0	2.7 ± 1.0
CALCINATED	1.7 ± 0.7	2.3 ± 1.0
ACTIVATED	1.1 ± 0.7	2.1 ± 1.7
APTES	2.4 ± 1.3	3.2 ± 1.7
APDES	2.1 ± 0.2	2.6 ± 0.3
APTES+APDES	2 ± 1.5	2.7 ± 2.1

Observing the results and the high standard deviations obtained, only a few qualitative considerations can be considered. Indeed, R_a and R_q show a decrease from the as-received fibers the calcinated and activated ones. When commercial sizing is removed by the calcination process and subsequent activation process (calcinated fibers subjected to an acid process for hydroxyl regeneration) smoother surfaces were obtained. These results are completely in accordance with other research about surface modification of glass fibers [31]. On the other hand, when aminosilane are applied on the fibers surfaces an increase in R_a and R_q is shown. The highest values of the roughness parameters obtained

for APTES coating is due to the high amount of organic matter deposited on the fiber surfaces. These results are in accordance with morphologic and topographic observations carried out by SEM and AFM and showed in [12]. A higher surface roughness observed for fibers treated with the trifunctional silane might contribute to improve the adhesion between the fiber and the matrix by mechanical adhesion, acting surface heterogeneities as mechanical attachment points. However, no correlation can be found from SEM fractographic analysis nor the mechanical behavior of the samples. Therefore, the roughness differences of the surfaces observed at nanoscale do not seem to be a significant factor influencing the final adhesion and mechanical performance of the cement-based composites.

4. CONCLUSIONS

The obtained results by mechanical tests shown that the presence of the new treated basalt fibers improves performance in cement-based mortars.

Indeed, the results by three-point flexural test underlined a better performance for samples containing activated (ACT+CEM) and APTES+APDES basalt fibers (APTAPD+CEM). An explication of this behavior can be related to the presence of high number of OH groups and/or easier accessibility to those OH on the fibers, enhancing the interaction with the cement matrix and preventing fiber sliding in the matrix. Especially, the flexural results obtained for the APTES+APDES basalt fibers and cement matrix confirmed higher compatibility and, consequently, a lesser brittle behavior with an increase in the flexural strength and toughness values.

About the compressive behavior, no relevant changes compared to the neat mortar were observed, but a slightly higher compressive strength values were obtained for samples containing activated (ACT+CEM) and silanized APTES (APT+CEM) and APTES+APDES (APTAPD+CEM) basalt fibers. Again, a higher accessibility of the OH groups generated by the activation process or given by the non-condensed silanol seems to induce a better compatibility with the cement matrix.

About the efficiency of the new treatments, fractographic analysis evidenced more cohesive failure mechanism for the samples containing activated (ACT+CEM) and APTES+APDES (APTAPD+CEM) basalt fibers. Indeed, from the SEM images of the failures it was observed better adhesion between the reinforcement and the matrix using new silanized fibers or simply activated fibers for their higher polar interaction according to the mechanical behavior. Profilometry measurements have demonstrated that more tortuous fracture surfaces are evident for the mortars containing fibers which supports less brittle behavior when basalt fibers are within the cement. Roughness differences at nanoscale of the basalt fibers surfaces do not seem to influence the final adhesion and mechanical performance of the cement-based composites.

Based on the obtained result, a good adhesion and consequently better mechanical performance were obtained for the mortars reinforced with basalt fibers treated with the mixture of the two silanes (APTES + APDES). The easier accessibility to the OH groups in their chemical structure can be responsible of stronger specific physico-chemical interactions with cement matrix inducing consequently better compatibility in terms of fiber-matrix adhesion.

In addition, the presence of a surface coating based on aminosilanes could contribute further to improve this adhesion due to interactions by hydrogen bonds between the amino groups ($-NH_2$) and the cement matrices.

ACKNOWLEDGEMENTS

This work was financially supported by the Projects MAT2014-59116-C2 (Ministerio de Economía y Competitividad); 2012/00130/004 (Fondos de Investigación de Fco. Javier GonzalezBenito, política de reinversión de costes generales, Universidad Carlos III de Madrid) and 2011/00287/002 (Acción Estratégica en Materiales Compuestos Poliméricos e Interfases, Universidad Carlos III de Madrid). The research was financially supported also by the Project “Bando per il Finanziamento di Progetti di Ricerca Congiunti per la Mobilità all’Estero di Studenti di Dottorato” prot. n° 0051266 (Università degli Studi di Roma, *La Sapienza*) in the frame the PhD Thesis of Morena Iorio. Finally, the authors

would like to thank the group In-service Material Performance (Universidad Carlos III de Madrid) for supporting the project in the mechanical tests.

REFERENCES:

[1] D.W. Fowler, Repair materials for concrete structures, in: N. Delatte (Ed.), Fail. Distress Repair Concr. Struct., Woodhead Publishing Limited, 2009: pp. 194–207. doi:10.1533/9781845697037.2.194.

[2] A.M. Brandt, Fibre reinforced cement-based (FRC) composites after over 40 years of development in building and civil engineering, Compos. Struct. 86 (2008) 3–9. doi:10.1016/j.compstruct.2008.03.006.

[3] K. Raoufi, J. Weiss, The role of fiber reinforcement in mitigating shrinkage cracks in concrete, in: R. Fangueiro (Ed.), Fibrous Compos. Mater. Civ. Eng. Appl., Woodhead Publishing Limited, 2011: pp. 168–188. doi:10.1016/B978-1-84569-558-3.50006-5.

[4] M.E. Arslan, Effects of basalt and glass chopped fibers addition on fracture energy and mechanical properties of ordinary concrete: CMOD measurement, Constr. Build. Mater. (2016). doi:10.1016/j.conbuildmat.2016.03.176.

[5] S.P. Shah, C. Ouyang, Mechanical behavior of fiber- reinforced cement-based composites, J. Am. Ceram. Soc. 74 (1991) 2947–2953. doi:https://doi.org/10.1111/j.1151-2916.1991.tb06836.x.

[6] C.D. Johnston, Fiber-Reinforced Cements and Concretes, in: Adv. Concr. Technol., Taylor & F, Taylor & Francis Group, 2001: p. Volume 3.

[7] V. Fiore, T. Scalici, G. Di Bella, A. Valenza, A review on basalt fibre and its composites, Compos. Part B Eng. 74 (2015) 74–94. doi:10.1016/j.compositesb.2014.12.034.

[8] L.R. Betterman, C. Ouyang, S.P. Shah, Fiber-matrix interaction in microfiber-reinforced mortar, Adv. Cem. Based Mater. 2 (1995) 53–61. doi:10.1016/1065-7355(95)90025-X.

[9] L. Li, Z. Xia, Role of interfaces in mechanical properties of ceramic matrix composites, Adv. Ceram. Matrix Compos. Second Ed. (2018) 355–374. doi:10.1016/B978-0-08-102166-8.00015-3.

[10] V.A. Rybin, A. V. Utkin, N.I. Baklanova, Alkali resistance, microstructural and mechanical performance of zirconia-coated basalt fibers, Cem. Concr. Res. 53 (2013) 1–8. doi:10.1016/j.cemconres.2013.06.002.

[11] Y.M. Abbas, M. Iqbal Khan, Fiber–Matrix Interactions in Fiber-Reinforced Concrete: A Review, Arab. J. Sci. Eng. 41 (2016) 1183–1198. doi:10.1007/s13369-016-2099-1.

[12] M. Iorio, M.L. Santarelli, G. González-Gaitano, J. González-Benito, Surface modification and characterization of basalt fibers as potential reinforcement of concretes, Appl. Surf. Sci. 427 (2018) 1248–1256. doi:10.1016/j.apsusc.2017.08.196.

[13] R.D. Tolêdo Filho, K. Ghavami, G.L. England, K. Scrivener, Development of vegetable fibre-mortar composites of improved durability, Cem. Concr. Compos. 25 (2003) 185–196.

doi:10.1016/S0958-9465(02)00018-5.

[14] R. Ralegaonkar, H. Gavali, P. Aswath, S. Abolmaali, Application of chopped basalt fibers in reinforced mortar: A review, Constr. Build. Mater. 164 (2018) 589–602. doi:10.1016/j.conbuildmat.2017.12.245.

[15] J. Branston, S. Das, S.Y. Kenno, C. Taylor, Mechanical behaviour of basalt fibre reinforced concrete, Constr. Build. Mater. 124 (2016) 878–886. doi:10.1016/j.conbuildmat.2016.08.009.

[16] C. Jiang, K. Fan, F. Wu, D. Chen, Experimental study on the mechanical properties and microstructure of chopped basalt fibre reinforced concrete, Mater. Des. 58 (2014) 187–193. doi:10.1016/j.matdes.2014.01.056.

[17] C. High, H.M. Seliem, A. El-Safty, S.H. Rizkalla, Use of basalt fibers for concrete structures, Constr. Build. Mater. (2015). doi:10.1016/j.conbuildmat.2015.07.138.

[18] M.L. Santarelli, F. Sbardella, M. Zuena, M. Albé, G. Quattrociocchi, J. Tirilló, M. Valente, F. Sarasini, Malte più performanti con le fibre di basalto, Compos. Mag. 33 (2014) 7–16. http://hdl.handle.net/10278/44412.

[19] Z.C. Girgin, M.T. Yıldırım, Usability of basalt fibres in fibre reinforced cement composites, Mater. Struct. Constr. 49 (2016) 3309–3319. doi:10.1617/s11527-015-0721-4.

[20] E. Standard, EN 197-1 Cement. Part 1: Composition, specifications and conformity criteria for common cements, (2011).

[21] E. Standard, EN 196-1 Methods of testing cement. Part 1: Determination of strength, (2005) 1–33.

[22] E. Standard, EN 1015-11 Methods of test for mortar for masonry. Part 11: Determination of flexural and compressive strength of hardened mortar, (2000).

[23] M. Tiryakioğlu, D. Hudak, G. Ökten, On evaluating Weibull fits to mechanical testing data, Mater. Sci. Eng. A. 527 (2009) 397–399. doi:10.1016/j.msea.2009.08.014.

[24] A. Saghafi, A.R. Mirhabibi, G.H. Yari, Improved linear regression method for estimating Weibull parameters, Theor. Appl. Fract. Mech. 52 (2009) 180–182. doi:10.1016/j.tafmec.2009.09.007.

[25] J. Gonzalez-Benito, J. Martinez-Tarifa, M.E. Sepúlveda-García, R.A. Portillo, G. Gonzalez-Gaitano, Composites based on HDPE filled with BaTiO3 submicrometric particles. Morphology, structure and dielectric properties, Polym. Test. 32 (2013) 1342–1349. doi:10.1016/j.polymertesting.2013.08.012.

[26] A. Nevarez-Rascon, A. Aguilar-Elguezabal, E. Orrantia, M.H. Bocanegra-Bernal, Compressive strength, hardness and fracture toughness of Al 2O3 whiskers reinforced ZTA and ATZ nanocomposites: Weibull analysis, Int. J. Refract. Met. Hard Mater. 29 (2011) 333–340. doi:10.1016/j.ijrmhm.2010.12.008.

[27] J.B. Quinn, G.D. Quinn, A practical and systematic review of Weibull statistics for reporting strengths of dental materials, Dent. Mater. 26 (2010) 135–147. doi:10.1016/j.dental.2009.09.006.

[28] J.N. Miller, J.C. Miller, Statistics and Chemometrics for Analytical Chemistry, Sixth Edit, Pearson Education Limited, 2010.

[29] M. Iorio, D. Olmos, M.L. Santarelli, J. González-benito, Applied Surface Science Fluorescence study of the hydrolytic degradation process of the polysiloxane coatings of basalt fi bers, Appl. Surf. Sci. 475 (2019) 754–761. doi:10.1016/j.apsusc.2018.12.223.

[30] M.A. Issa, M.A. Issa, M.S. Islam, A. Chudnovsky, Fractal dimension-a measure of fracture roughness and toughness of concrete, Eng. Fract. Mech. 70 (2003) 125–137. doi:10.1016/S0013-7944(02)00019-X.

[31] S.G. Turrión, D. Olmos, J. González-Benito, Complementary characterization by fluorescence and AFM of polyaminosiloxane glass fibers coatings, Polym. Test. 24 (2005) 301–308. doi:10.1016/j.polymertesting.2004.11.006.